

# NJC

Accepted Manuscript



This is an *Accepted Manuscript*, which has been through the Royal Society of Chemistry peer review process and has been accepted for publication.

*Accepted Manuscripts* are published online shortly after acceptance, before technical editing, formatting and proof reading. Using this free service, authors can make their results available to the community, in citable form, before we publish the edited article. We will replace this *Accepted Manuscript* with the edited and formatted *Advance Article* as soon as it is available.

You can find more information about *Accepted Manuscripts* in the [Information for Authors](#).

Please note that technical editing may introduce minor changes to the text and/or graphics, which may alter content. The journal's standard [Terms & Conditions](#) and the [Ethical guidelines](#) still apply. In no event shall the Royal Society of Chemistry be held responsible for any errors or omissions in this *Accepted Manuscript* or any consequences arising from the use of any information it contains.

## ARTICLE

# Porous Framework Based on Tetrakis(4-pyridyloxy methyl)methane Fine-tuned by Metal Ions: Synthesis, Crystal Structures and Adsorption Properties

Cite this: DOI: 10.1039/x0xx00000x

Zhao Li,<sup>a</sup> Xi Chen,<sup>a</sup> Fan Yu,<sup>b</sup> Min Su,<sup>a</sup> Bi-quan Zhang,<sup>a</sup> Bao Li,<sup>a,\*</sup> Tian-le Zhang<sup>a,\*</sup>

Received 00th January 2012,  
Accepted 00th January 2012

DOI: 10.1039/x0xx00000x

www.rsc.org/

**Abstract:** Solvothermal reactions of tetrakis(4-pyridyloxymethyl)methane (TPOM) and 4,4'-oxybisbenzoic acid (H<sub>2</sub>oba) with different metal ions under different synthesis temperature produced three new coordination polymers (CPs), namely, {[Co<sub>2</sub>(TPOM)(oba)<sub>2</sub>(H<sub>2</sub>O)<sub>2</sub>]}<sub>n</sub> (**1**), {[Zn<sub>2</sub>(TPOM)(oba)<sub>2</sub>]}<sub>n</sub> (**2**) and {[Cd<sub>2</sub>(TPOM)(oba)<sub>2</sub>(H<sub>2</sub>O)<sub>2</sub>]}<sub>n</sub> (**3**). **1** and **3** present similar topological structure which could be analyzed by two different ways. **2** exhibits a rare porous structure assembled by tetra-pyridinate ligand TPOM. The luminescent properties of **2** and **3** as well as the corresponding sample immersed in different solvents had been investigated, which suggested the potential application in luminescent sensing. In addition, the dyes and iodine adsorption properties of activated sample of **2** were also investigated. All of the results indicate that the proper selection of metal ions and auxiliary ligands plays the important roles in constructing porous coordination polymers.

## Introduction

Considerable attention on coordination polymers (CPs), especially porous CPs (PCPs), stems from not only their intrinsic topological network but potential applications as molecular separation, magnetism, chiral catalysis, gas storage and photo-luminescent properties.<sup>1-5</sup> However, the controllable construction of CPs with desired properties still poses a great challenge, which might be caused by the complicated synthesis conditions as reaction temperature, pH value, solvent system, and metal ions.<sup>6-11</sup> Comparably, proper design and selection of organic linkers with modifiable backbone and high connectivity would be of facile route to modulate novel network topologies with anticipated properties,<sup>12</sup> which have been validated by various carboxyl ligands.<sup>13</sup> In contrast, CPs constructed by highly-connected flexible N-bridging ligands are relatively limited. Tetrakis(4-pyridyloxymethyl) methane (TPOM) exhibits variable configurations because the pyridyl arms could twist around the central quaternary carbon atom randomly. Various CPs that exhibit different topologies and functional properties have been explored by our group and other ones, in which dense packing structures were usually presented.<sup>14</sup> In contrast, the relevant PCPs were rarely reported that might be caused by the flexible configuration of tetra-pyridinate ligand.

To rationally construct porous framework containing this flexible tetra-pyridyl ligand, the proper selection of auxiliary carboxyl ligands might be of the important key. The auxiliary ligands that exhibit effective length and specific rigid connection mode would be facile to result in porous framework with TPOM. For example, utilizing the bent 4,4'-(Hexafluoroisopropylidene)bis(benzoic acid) (H<sub>2</sub>hfipbb)

reacted with cadmium and TPOM, three novel interpenetrated polymers were obtained, and porous structure of single skeleton truly presented even the pores are blocked by the same skeletons. Inspired by this idea, a bent dicarboxyl ligand, 4,4'-oxybisbenzoic acid (H<sub>2</sub>oba), was selected to try to assemble the PCPs with TPOM ligand.<sup>15</sup> Compared to H<sub>2</sub>hfipbb, H<sub>2</sub>oba has no sites as F atoms to form the intricate interactions with other skeleton, which might generate unique porous architectures. With all the above considerations in mind, we reported the synthesis and characterization of three novel CPs assembled from the tetra-pyridines linker, H<sub>2</sub>oba and series of metal cations under different synthesis temperature, namely, {[Co<sub>2</sub>(TPOM)(oba)<sub>2</sub>(H<sub>2</sub>O)<sub>2</sub>]}<sub>n</sub> (**1**), {[Zn<sub>2</sub>(TPOM)(oba)<sub>2</sub>]}<sub>n</sub> (**2**) and {[Cd<sub>2</sub>(TPOM)(oba)<sub>2</sub>(H<sub>2</sub>O)<sub>2</sub>]}<sub>n</sub> (**3**). The new compounds are characterized by elemental analysis, IR spectra, and X-ray crystallography. Crystal structures, topological analyses of these compounds are presented in detail.

## Results and discussion

### Crystal structure of 1

Compound **1** crystallizes in the monoclinic space group *C2/c*, and the asymmetric unit, shown in Figure 1, contains two Co atoms, one complete tetra-pyridine ligand and two deprotonated dicarboxyl ligands. Each of the Co atom could be considered as penta-coordinate environment with its coordination sphere being a slightly distorted trigonal bipyramid, which is surrounded by one coordinated aqua molecule, two pyridyl N atoms of different TPOM ligands and two different types of carboxyls exhibited mono-dentate and chelated modes. The Co-

N and Co-O bond lengths range from 2.048(2) to 2.313(3) Å, in accordance with the reported Co<sup>II</sup>-N or -O bond lengths.

Table 1 crystal data of 1 -3

	1	2	3
formula	C <sub>53</sub> H <sub>48</sub> Co <sub>2</sub> N <sub>4</sub> O <sub>16</sub>	C <sub>59</sub> H <sub>70</sub> N <sub>6</sub> O <sub>24</sub> Zn <sub>2</sub>	C <sub>53</sub> H <sub>48</sub> Cd <sub>2</sub> N <sub>4</sub> O <sub>16</sub>
Formula Mass	1114.75	1377.99	1221.71
Crystal system	Monoclinic	Monoclinic	Monoclinic
a/Å	47.02(6)	18.894(4)	46.403
b/Å	10.771(7)	20.963(4)	11.125
c/Å	23.78(3)	22.381(5)	24.144
β/°	94.87(6)	114.95(3)	98.48
volume/Å <sup>3</sup>	12000(23)	8037(3)	12327.7
Space group	C2/c	C2/c	C2/c
Z	8	4	8
Final R1 values	0.0926	0.1341	0.0710
Final R1 values	0.1626	0.1499	0.1618

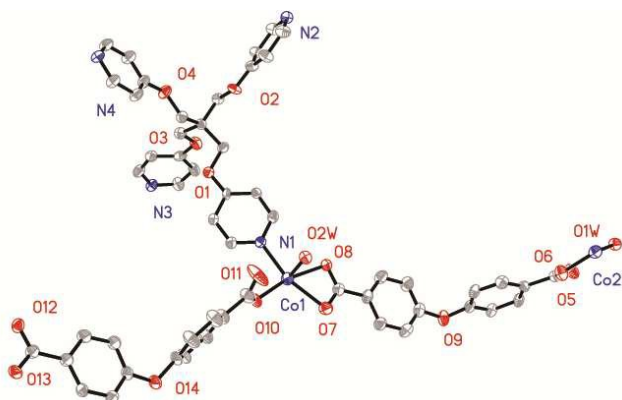


Figure 1. ORTEP drawing (30% probability) of the asymmetric unit of 1 along with the atom numbering scheme. (H atoms were omitted for clarity)

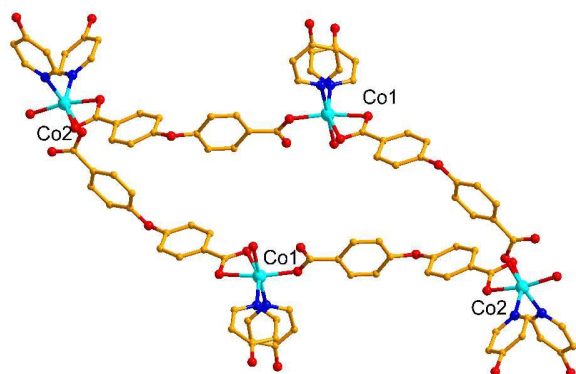


Figure 2. the perspective view of the circle structure of tetra-cobalt ions formed by the di-carboxyl ligand.

For 1, oxa connects two cobalt ions by its two carboxyl groups in different coordination mode: monodentate and chelate mode. In this way, a tetra-cobalt circle is formed by the connection of four oxa ligands, which is further stabilized by eight TPOM ligands, shown in figure 2. The inherently flexible tetrapyrridyl ligand TPOM adopts a highly distorted tetrahedral disposition of the four pyridyl groups, each of which connects a distinct Co atom with N...C<sub>central</sub>...N angles ranging from 110.47(12)° to 133.43(11)° (two Co1 atoms and two Co2 atoms). In other way, each TPOM ligand connects four tetracobalt circles, shown in figure 3. As such, a 3D packing crystal structure is formed.

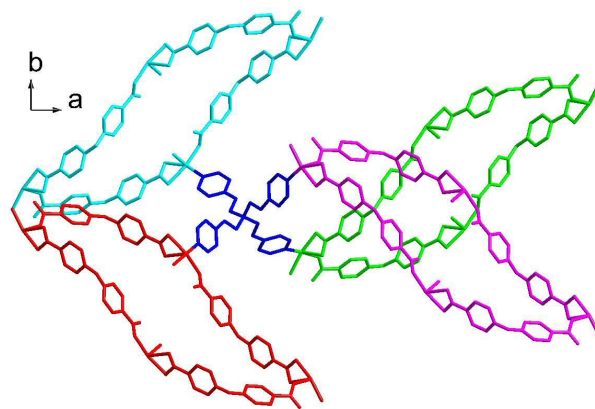


Figure 3. the perspective view of the coordination mode of TPOM.

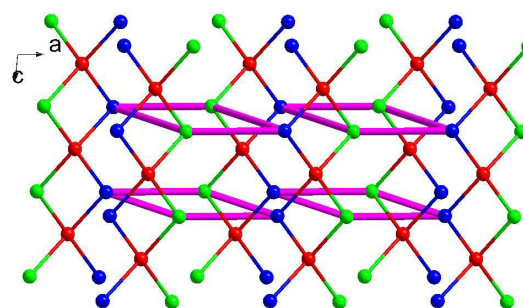


Figure 4. the view of the 3D structure of complex 1 in a simplified ball-and-stick model: the red, green and blue balls represent the 4-connected TPOM ligands, Co1 atoms and Co2 atoms, respectively.

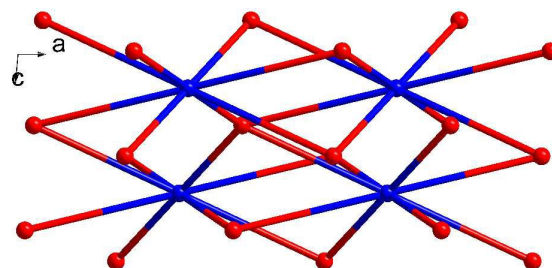


Figure 5. the view of the 3D structure of complex 1 in a simplified ball-and-stick model: the red and blue balls represent the 4-connected TPOM ligands and eight-connected tetra-cobalt circles, respectively.

In order to fully investigate the topological structure of 1, the topological structure of 1 was analyzed in two different ways: 1) Generally, considering two types of crystallographically distinct cobalt ions, oxa ligands and TPOM ligands as four-, two- and four-connecting nodes, the overall structure of 1 topologically possesses a novel 4,4,4-connected 3-nodal net with the point (Schläfli) symbol  $\{4^2 \cdot 10^4\} \{4^2 \cdot 6^2 \cdot 8^2\}_2$  calculated with TOPOS software (figure 4).<sup>16</sup> This net was simplified to analyze supernet-subnet relations by TOPOS as subnet of the 4,4,4-connected topology, and has never been observed in CPs. 2) considering the tetra-cobalt circles and TPOM ligands as four- and eight-connecting nodes, the overall structure of 1 topologically possesses a novel 4,8-connected 2-nodal net with the point (Schläfli) symbol  $\{4^{12} \cdot 8^{16}\} \{4^2 \cdot 8^4\}_2$  calculated with TOPOS software. This net was simplified to analyze supernet-subnet relations by TOPOS as subnet of the 4,8-connected

topology, and has never been observed in CPs (figure 5). Therefore, two novel topological symbols had been presented, which are helpful to give the complements in topological structures.

### Crystal structure of 3

By utilizing the cadmium ion, a new polymer presented similar topological structure of **1** was obtained. Compound **3** also crystallizes in the monoclinic space group  $C2/c$ , and the asymmetric unit, shown in Figure 6, contains two Cd atoms, one complete tetra-pyridine ligand and two deprotonated dicarboxyl ligands. Each of the Cd atoms could be considered as penta-coordinate environment with its coordination sphere being a slightly distorted trigonal bipyramid, which is surrounded by one coordinated aqua molecule, two pyridyl N atoms of different TPOM ligands and two different types of carboxyls exhibited mono-dentate and chelated modes. The Cd-N and Cd-O bond lengths range from 2.193(2) to 2.477(3) Å, in accordance with the reported  $Cd^{II}$ -N or -O bond lengths. Similar tetra-nuclear ring is also formed only by oxa ligands, which is further interconnected by TPOM ligands with the  $N \cdots C_{\text{central}} \cdots N$  angles ranging from 90.68(12)° to 115.16(11)° to form the 3D structure. Topological and XRD experiment reveal that **3** presents the similar structure with **1**. Calculated using the PLATON routine, the solvent accessible volume in the dehydrated structure of **3** is about 22.4%. The larger volume effect of Cd ion must be responsible for the porous structure of **3** compared to Co ion in **1**.

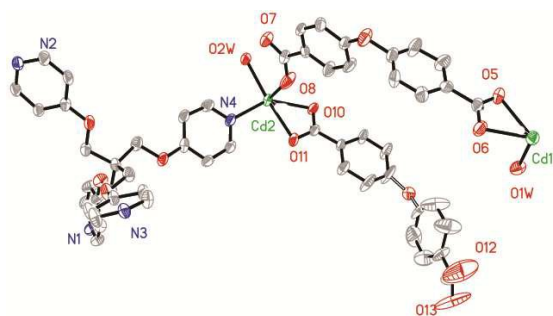


Figure 6. ORTEP drawing (30% probability) of the asymmetric unit of **3** along with the atom numbering scheme. ( H atoms were omitted for clarity )

### Crystal structure of 2

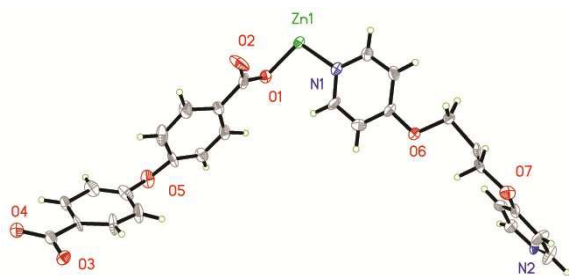


Figure 7. ORTEP drawing (30% probability) of the asymmetric unit of **2** along with the atom numbering scheme.

Substituting the cobalt ion by zinc ion, a distinct structure was formed. Compound **2** also crystallizes in the monoclinic space group  $C2/c$ , and the asymmetric unit, shown in Figure 7, contains one Zn atom, half tetra-pyridine ligand and one

deprotonated dicarboxyl ligand. Each of the Zn atom could be considered as tetra-coordinate environment with its coordination sphere being a slightly distorted tetrahedron, which is surrounded by two pyridyl N atoms of different TPOM ligands and two monodentate carboxyls from two oxa ligands. The Zn-N and Zn-O bond lengths range from 1.934(2) to 2.052(3) Å, in accordance with the reported  $Zn^{II}$ -N or -O bond lengths.

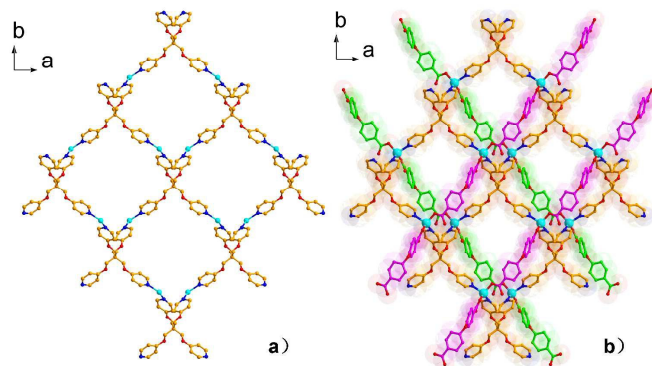


Figure 8. a) the perspective view of the 2D layer of **2** constructed only by zinc ions and TPOM ligands; b) 3D packing structure of **2** along  $c$ -axis direction.

For **2**, The inherently flexible tetrapyridyl ligand TPOM adopts a highly distorted tetrahedral disposition of the four pyridyl groups, each of which connects a distinct Zn atom with  $N \cdots C_{\text{central}} \cdots N$  angles ranging from 92.51(12)° to 115.22(11)° to form the 2D layer structure in  $ab$  plane ( figure 8 ). In addition, oxa ligands bridged two zinc ions via its two mono-dentate carboxyls, and capped onto the sides of 2D zinc-TPOM layer. As such, a tape-like structure composed of two layers of zinc atoms with coordinated oxa ligands and one “sandwiched” layer of 4-connected bridging TPOM ligands is assembled. Square-shaped pores can be clearly identified along the crystallographic  $c$ -axis after the pack of “sandwiched” layer ( Figure 8 ). Calculated using the PLATON routine, the solvent accessible volume in the dehydrated structure of **2** is about 49.9%.

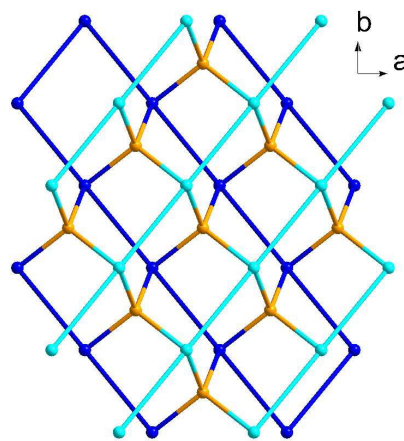


Figure 9. the view of the 3D structure of complex **2** in a simplified ball-and-stick model: the yellow and dark and light blue balls represent the 4-connected TPOM and cobalt ions, respectively.

Considering the zinc ions, oxa ligands and TPOM ligands as four-, two- and four-connecting nodes, the overall structure of **2** topologically possesses a novel 4,4-connected 2-nodal 4,4L35 net with the point (Schläfli) symbol  $\{5^4 \cdot 6^2\} \{5^5 \cdot 8\}_2$  calculated with *TOPOS* software (figure 9).<sup>16</sup>

### Thermal stability

The thermogravimetric (TG) analysis was performed in  $N_2$  atmosphere on polycrystalline samples of complexes **1-3** and the TGA curves are shown in Figure S1. The TGA curve of **1** shows the first weight loss of 10 % in the temperature range of 25 – 120 °C, which indicates the loss of lattice molecules per formula unit. The metal–organic framework retains until 370 °C, and then starts to decompose accompanying loss of organic ligands. Similar thermal stability of **3** could be observed, which is assigned to the loss of aqua molecules. For **2**, the quick weight loss from 20 to 120 °C attributed to the release of guest molecules, then the framework retains in the temperature range of 70–350 °C, and then decompose. The thermal stability of these CPs must be assigned to the highly-connected mode between the organic ligands and metal ions.

### Luminescent properties of **2** and **3**

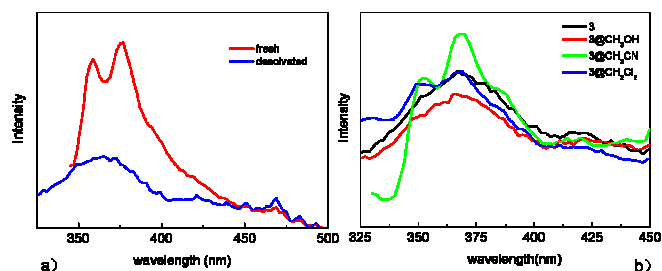


Figure 10. luminescent properties of fresh and desolvated sample of **2** (a), and fresh sample and sample containing different solvents of **3** (b).

The luminescent properties of **2** and **3** were investigated in the solid state at room temperature. Compared to the free ligand TPOM and  $H_2oba$ ,<sup>14,15</sup> **2** exhibits two peaks at 360 and 380 nm, which might originate from ligand-to-metal charge transitions (figure 10a). Comparably, the desolvated samples were immersed in different solvent, and only one peak at 370 nm were observed. XRD analysis reveals that the whole framework of desolvated sample is still stable (figure S2), and the variable luminescent properties might be ascribed to the effect of lattice molecules. However, complex **3** exhibits one peak at around 370 nm (figure 10b) which might be assigned to ligand-to-metal charge transfer. In addition, the desolvated sample was also immersed in different solvents, and different luminescent properties were observed. Desolvated sample and **3**@CH<sub>3</sub>OH exhibits similar luminescent properties with fresh sample. However, one additional peak at 350 nm was observed for **3**@CH<sub>3</sub>CN and **3**@CH<sub>2</sub>Cl<sub>2</sub>. XRD analysis reveals that the whole framework of desolvated sample and ones with different solvents are still stable ( Figure S3 ). Therefore, the different interactions between the framework and guest molecules must be responsible for the variable luminescent properties.

### Dyes and Iodine Uptake of **2**

Usually, highly porous structure would be collapsed due to the internal stress originated from the process of drying porous productions. Therefore, nitrogen or argon physisorption that requires activation in vacuum could not be of the essential

choice for determining the porosity of the materials used for catalytic or absorption applications in solution. Thus, to prove the permanent porosity and accessibility for larger molecules of **2**, three different dye molecules were adsorbed in solution. When refreshed **2** were soaked in  $CH_2Cl_2$  solutions of different kinds of dyes, dye molecules could be efficiently adsorbed over a period of time and the colorless crystals rapidly became colored. The adsorptivity of compounds **2** is 0.35 mg/g for Basic Red 2, 0.5 mg/g for Crystal Violet, and 0.56 mg/g for Methylene Blue 9. The possibilities of absorbing dye molecules were further evaluated by solid Uv-Vis spectroscopy (Figure 11), which confirms the incorporation of dye molecules into the parent structure of **2**. In this way, the porous structure of **2** in solution could be validated.

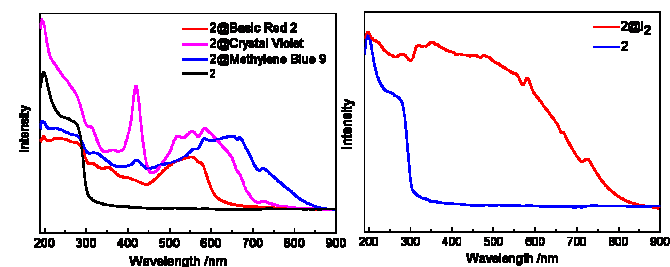


Figure 11. Uv-Vis spectra of adsorption of different dyes and  $I_2$  within the pores of **2**.



Figure 12. The photo of  $I_2$  ( 5 mmol/L ) uptake of **2** in cyclohexane solution with different time.

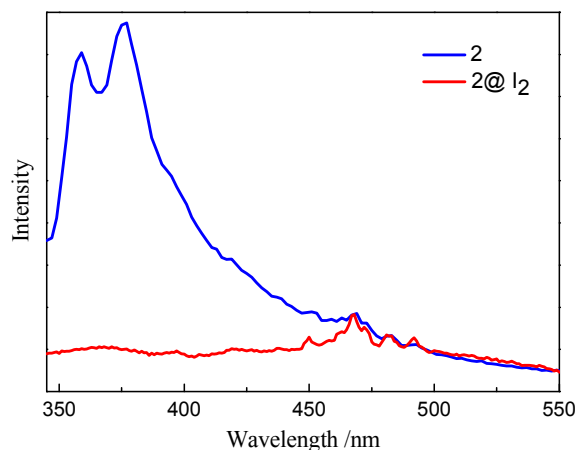


Figure 13. the luminescent properties of **2**@ $I_2$ .

In addition, the capabilities of iodine adsorption were then tested samples of activated **2** after soaked in methanol. After immersion in cyclohexane solution of  $I_2$  for 5h, the products became brown (Figure 12), which could not return to the original color when washed with cyclohexane.

The iodine uptake of **2** was examined by the gravimetric measurements taken after 48h revealed that the mass of **2** increased by 15wt % . Uv-Vis spectra in the solid states of **2**@I<sub>2</sub> showed corresponding peaks compared to the fresh sample. Meanwhile, the luminescent properties of **2**@I<sub>2</sub> became different compared to the fresh sample. The peaks around 375nm were quenched by including iodine into the framework (Figure 13). When the crystalline solids of **2**@I<sub>2</sub> were soaked in methanol for 5h, the color of the solids changed from brown to yellow, and the color of the methanol solution deepened gradually from colorless to yellow, which explained that the sorption and desorption of I<sub>2</sub> are not completely reversible.

## Conclusion

In conclusion, by proper selection of metal ions and auxiliary V-shaped carboxyl ligands, three CPs have been synthesized and characterized structurally. Both **1** and **3** show tetra-nuclear circle connected by oxa ligands, and 3D novel topological net constructed by the joint of TPOM and tetra-nuclear circle. In contrast, **2** exhibits 1D chains connected by oxa ligands, and 2D framework with 1D channels in lattice by the connection of TPOM. In addition, **2** presents the corresponding dyes and iodine adsorption properties, which validate the porosity of **2**. Therefore, the coordination environment of metal ion and connection mode of auxiliary carboxyl ligands play the important roles in constructing PCPs with TPOM ligands. The continuous work is still focusing on pursuing PCPs by utilizing the different auxiliary ligands and metal ions with multi-N ligands and investigating their corresponding adsorption properties.

## Acknowledgements

We gratefully acknowledge the National Natural Science Foundation of China (no.21471062, 21101066), Wuhan Science and Technology Bureau (no. 201271031384 ) and ) for financial support, and the Analytical and Testing Center, Huazhong University of Science and Technology for analysis and spectral measurements.

## Notes and references

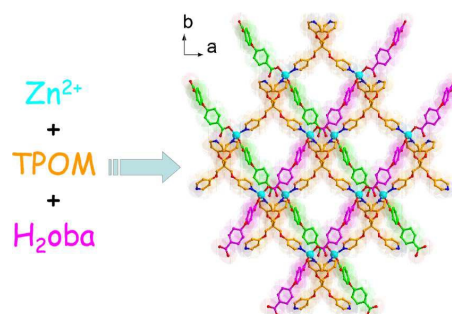
<sup>a</sup> Key Laboratory for Large-Format Battery Materials and System, College of Chemistry and Chemical Engineering, Huazhong University of Science and Technology, Wuhan, Hubei 430074, P. R. China

<sup>b</sup> Key Laboratory of Optoelectronic Chemical Materials and Devices of Ministry of Education, School of Chemical and Environmental Engineering, Jiangnan University, Wuhan 430056, P. R. China

Electronic Supplementary Information (ESI) available: Detailed synthesis, XRD, TGA, Photo and an X-ray crystallographic file in cif format for 1-3. See DOI: 10.1039/b000000x/

- M. O'Keeffe and O. M. Yaghi. *Chem. Rev.*, 2012, **112**, 675; O. M. Yaghi, H. Furukawa, *J. Am. Chem. Soc.*, 2009, **131**, 8875; Y. Q. Huang, B. Ding, H. B. Song, B. Zhao, P. Ren, P. Cheng, H. G. Wang, D. Z. Liao, S. P. Yan, *Chem. Commun.*, 2006, 4906; Y. Cui, Y. Yue, G. Qian, and B. Chen. *Chem. Rev.*, 2012, **112**, 1126; N. Stock and S. Biswas. *Chem. Rev.*, 2012, **112**, 933. H.-L. Jiang, Y. Tatsu, Zh.-H. Lu and Q. Xu. *J. Am. Chem. Soc.*, 2010, **132**, 5586.
- K. S. Gavrilenko, S. V. Punin, O. Cador, S. Golhen, L. Ouahab and V. V. Pavlishchuk, *J. Am. Chem. Soc.*, 2005, **127**, 12246; J. W. Zhao, J. Zhang, S. T. Zheng and G. Y. Yang, *Chem. Commun.*, 2008, 570; F. Yu, D. Li, L. Cheng, Z. Yin, M. Zeng and M. Kurmoo, *Inorg. Chem.* 2015, **54**, 1655.
- H. Cho, B. Ma, S. T. Nguyen, J. T. Hupp, A. T. E. Schmitt, *Chem. Commun.*, 2006, 2563 ; L. S. Long, Y. R. Wu, R. B. Huang, L. S. Zheng, *Inorg. Chem.*, 2004, **43**, 3798.
- G. Férey, M. Latroche, C. Serre, F. Millange, T. Loiseau and A. P. Guégan, *Chem. Commun.*, 2003, 2976; Y. Zhang, W. Zhang, F. Feng, J. P. Zhang and X. M. Chen, *Angew. Chem., Int. Ed.* 2009, **48**, 5287.
- J. Li, R. J. Kuppler and H. Zhou, *Chem. Soc. Rev.*, 2009, **38**, 1477; B. Li, L. Chen, R. Wei, J. Tao, R. Huang, L. Zheng and Z. Zheng, *Inorg. Chem.*, 2011, **50**, 424.
- M. Tong, S. Kitagawa, H. Chang and M. Ohba, *Chem. Commun.*, 2004, 418; Y. Dong, Y. Jiang, J. Li, J. Ma, F. Liu, B. Tang, R. Huang and S. R. Batten, *J. Am. Chem. Soc.*, 2007, **129**, 4520; M. Dan and C. N. R. Rao, *Angew. Chem. Int. Ed.*, 2006, 45, 281.
- P. Zhang, B. Li, Y. Zhao, X. Meng and T. L. Zhang, *Chem. Commun.*, 2011, **47**, 7722; M. Zuhayra, W. U. Kampen, E. Henze, Z. Soti, L. Zsolnai, G. Huttner and F. A. Oberdorfer, *J. Am. Chem. Soc.*, 2006, **128**, 424; D. Sun, H. Xu, C. Yang, Z. Wei, N. Zhang, R. Huang and L. Zheng, *Cryst. Growth Des.*, 2010, **10**, 4642.
- Y. Zou, M. Park, S. Hong and M. S. Lah, *Chem. Commun.*, 2008, 2340; B. Zheng, J. F. Bai, J. Duan, L. Wojtas, and M. J. Zaworotko, *J. Am. Chem. Soc.*, 2011, **133**, 748; D. Zhao, D. Yuan, D. F. Sun and H.-C. Zhou, *J. Am. Chem. Soc.*, 2009, **131**, 9186.
- Q.-R. Fang, D.-Q. Yuan, J. Sculley, J.-R. Li, Z.-B. Han and H.-C. Zhou, *Inorg. Chem.*, 2010, **49**, 11637; H. K. Chae, D. Y. Siberio-Perez, J. Kim, Y. Go, M. Eddaoudi, A. J. Matzger, M. O'Keeffe and O. M. Yaghi, *Nature*, 2004, **427**, 523.
- D. Sun, S. Ma, Y. Ke, T. Petersen and H. Zhou, *Chem. Commun.*, 2005, 2663; K. C. Stylianou, R. Heck, S. Y. Chong, J. Bacsá, J. T. A. Jones, Y. Z. Khimiyak, D. Bradshaw and M. J. Rosseinsky, *J. Am. Chem. Soc.*, 2010, **132**, 4119.
- M. Dincă, A. Dailly and J. R. Long, *Chem. Eur. J.*, 2008, **14**, 10280.
- E. D. Bloch, D. Britt, C. Lee, C. J. Doonan, F. J. Uribe-Romo, H. Furukawa, J. R. Long and O. M. Yaghi, *J. Am. Chem. Soc.*, 2010, **132**, 14382; M. H. Zeng, Q. X. Wang, Y. X. Tan, S. Hu, H. X. Zhao, L. S. Long and M. Kurmoo, *J. Am. Chem. Soc.*, 2010, **132**, 2561.
- B. L. Chen, S. Q. Ma, F. Zapata, E. B. Lobkovsky and J. Yang, *Inorg. Chem.* 2006, **45**, 5718 ; H. Chun, D. N. Dybtsev, H. Kim and K. Kim, *Chem.-Eur. J.* 2005, **11**, 3521; H. L. Jiang, Y. Tatsu, Z. Lu and Q. Xu, *J. Am. Chem. Soc.*, 2010, **132**, 5586; W. Yang, X. Lin, A. J. Blake, C. Wilson, P. Hubberstey, N. R. Champness and M. Schröder, *Inorg. Chem.*, 2009, **48**, 11067.
- J. S. Hu, Y. J. Shang, X. Q. Yao, L. Qin, Y. Zh. Li, Z. J. Guo, H. G. Zheng and Z. L. Xue, *Cryst. Growth Des.*, 2010, **10**, 2676 ; S.-B. Ren, L. Zhou, J. Zhang, Y.-Zh. Li, H.-B. Du, and X.-Z. You, *CrystEngComm*, 2009, **11**, 1834; S.-B. Ren, L. Zhou, J. Zhang, Y.-L. Zhu, Y.-Zh. Li, H.-B. Du and X.-Z. You, *CrystEngComm.*, 2010, **12**, 1635; Q. Zhang, X. Bu, Z. Lin, T. Wu and P. Feng, *Inorg. Chem.*, 2008, **47**, 9724; J. Guo, J.-F. Ma, B. Liu, W.-Q. Kan and J. Yang, *Cryst. Growth Des.*, 2011, **11**, 3609; F. Yu and B. Li, *CrystEngComm*, 2011, **13**, 7025; F. Yu, W. Yu, B. Li and T. Zhang, *CrystEngComm*, 2012, **14**, 6770; F. Yu and B. Li, *CrystEngComm*, 2012, **14**, 6049; W. Yu, F. Yu, B. Li and T. Zhang, *CrystEngComm*,

- 2012, **14**, 8396; F. Yu, M. Xiang, A. Li, Y. Zhang and B. Li, *CrystEngComm*, 2015, **17**, 1556.
- 15 L. L. Liang, S. Ren, J. Zhang, Y. Zh. Li, H. B. Du and X. Z. You, *Cryst. Growth Des.*, 2010, **10**, 1307; J. Hu, X. Huang, C. Pan and L. Zhang, *Cryst. Growth Des.*, 2015, **15**, 2272.
- 16 V. A. Blatov, *IUCr CompComm Newsletter*, 2006, **7**, 4; see also <http://www.topos.ssu.samara.ru>.



Solvothermal reactions of tetrakis(4-pyridyloxymethyl)methane (TPOM) and 4,4'-oxybisbenzoic acid ( $H_2oba$ ) with different metal ions under different synthesis temperature produced three new coordination polymers. All of the results indicate that the proper selection of metal ions and auxiliary ligands plays the important roles in constructing porous coordination polymers.